Integrable aspects and soliton interaction for a generalized inhomogeneous Gardner model with external force in plasmas and fluids

Yu-Ping Liu,[1,2,*] Yi-Tian Gao,[1,†] and Guang-Mei Wei[3]

[1]*Ministry of Education Key Laboratory of Fluid Mechanics and National Laboratory for Computational Fluid Dynamics, Beijing University of Aeronautics and Astronautics, Beijing 100191, China*

[2]*School of Physics and Nuclear Energy Engineering, Beijing University of Aeronautics and Astronautics, Beijing 100191, China*

[3]*LMIB and School of Mathematics and System Sciences, Beijing University of Aeronautics and Astronautics, Beijing 100191, China*

(Received 26 April 2013; revised manuscript received 11 June 2013; published 20 November 2013)

A generalized inhomogeneous Gardner model with an external force term is investigated which can govern the soliton propagation and interaction in the vicinity of the negative ion critical density for certain plasmas or of equal layer depths for stratified fluids. Integrable aspects including the Lax pair and the Γ-Riccati-type Bäcklund transformation (Γ-R BT) are presented under the Painlevé conditions. By virtue of the Γ-R BT, analytic one- or two-soliton-like solutions with the inhomogeneous coefficients, external force term, eigenvalue in the Lax pair, and another parameter are obtained. Analytic analysis and graphic illustration imply that (1) the amplitude of a soliton is influenced by the quadratic and cubic nonlinear coefficients, the linear-damping coefficient, and the aforementioned eigenvalue; (2) the solitonic velocity is "controlled" by the inhomogeneous coefficients, the external force term, and the aforementioned eigenvalue and parameter; (3) the solitonic background is affected by the linear-damping coefficient, the external force term and the aforementioned parameter; and (4) the possibility of solitonic infection is dominated by the difference between eigenvalues.

DOI: 10.1103/PhysRevE.88.053204 PACS number(s): 05.45.Yv, 02.30.Ik, 52.35.Sb, 47.35.Fg

I. INTRODUCTION

The Korteweg-de Vries (KdV) model can describe the weakly nonlinear and weakly dispersive long waves in certain plasmas and fluid systems [1–8]. Experimentally observed solitons are slightly different from those via the KdV prediction due to the effect of finite ion temperature and higher-order nonlinearity [8–13]. At the critical density of the negative ion or low-temperature isothermal ions, for example, the higher-order nonlinear effect must be considered [9,12]. In the vicinity of the critical density, neither the KdV model nor the modified KdV (mKdV) model is sufficient for describing the ion wave or ion-acoustic wave [9–13]. In the ocean and atmosphere environments, nonlinearity is not so weak as to be implied by the KdV model [14]. In the next order of the perturbation, a higher-order KdV model can be obtained, which in general includes the cubic nonlinearity, the fifth-order linear dispersion, and the nonlinear dispersion [14–17]. For the internal waves in a two-layer fluid, when the pycnocline lies in the middle of fluid, the quadratic nonlinear term vanishes and the cubic nonlinear term makes the higher-order KdV model reduce to the mKdV model [14–23]. As a combination of the KdV-typed model with a quadratic nonlinearity term and the mKdV-typed model with a cubic nonlinear term, the generalized inhomogeneous Gardner model [24–27] is also called the combined KdV-mKdV [28–35] or extended KdV model [36–43], as follows:

$$q_t + a_1(t)qq_X + b_1(t)q^2q_X + c_1(t)q_{XXX} + d_1(t)q_X + f_1(t)q = 0, \quad (1)$$

where q is a wave function of the scaled space coordinate X and time coordinate t, the subscripts denote the partial derivatives, and the time-dependent analytic functions $a_1(t)$, $b_1(t)$, $c_1(t)$, $d_1(t)$, and $f_1(t)$ represent the quadratic nonlinear, cubic nonlinear, dispersive, dissipative, and linear-damping coefficients, respectively. For model (1), damping of the large-amplitude solitary waves with a small damping term has been investigated with both the analytic adiabatic asymptotic theory and numerical simulation [14], solitary-wave transformation with an asymptotic method and direct numerical simulation with a slowly varying cubic nonlinear coefficient have been studied [16], an auto-Bäcklund transformation (BT) and some kink-type solutions have been presented with the homogeneous balance [31] or truncated Painlevé expansion [38], respectively, and interaction between the breather and soliton has been provided by means of the Hirota bilinear method [41]. Model (1) with self-consistent sources and negative cubic nonlinear term has been studied by means of the generalized binary Darboux transformation [42]. Lax pair, BT, and N-soliton-like solutions of model (1) have also been presented [24]. Nontraveling solutions for model (1) with the aid of two first-order nonlinear ordinary differential equations have been obtained [25]. Based on the Hirota bilinear method, analytic N-soliton-like solutions of model (1) have been provided [26]. Transformations to convert model (1) to the constant-coefficient ones have been given [27]. Model (1) with the coefficients of time-dependent powers or nonlinear terms of any order has been investigated with the Lie symmetries and Painlevé analysis [44] or the bifurcation of dynamical systems [43].

In this work we will investigate the extension of model (1) with external forcing term $H(t)$ [45], i.e.,

$$u_t + a(t)uu_x + b(t)u^2u_x + c(t)u_{xxx} + d(t)u_x + f(t)u = H(t), \quad (2)$$

where u is a normalized wave function, and the time-dependent analytic functions $a(t)$, $b(t)$, $c(t)$, $d(t)$, and $f(t)$ represent the

*lyp@buaa.edu.cn

†gaoyt@public.bta.net.cn

quadratic nonlinear, cubic nonlinear, dispersive, dissipative, and linear-damping coefficients, respectively. Model (2) has been converted to the special case of model (1) with $a_1(t) = a(t) + 2b(t)\int H(t)\,dt$ and $d_1(t) = f_1(t) = 0$ by virtue of a Galilean-type transformation $u = \int H(t)\,dt + q$, $X(x,t) = x - \int\{d(t) + a(t)\int H(t)\,dt + b(t)[\int H(t)dt]^2\}\,dt$ and $T = t$, with the multisoliton solutions in possession of the Gaussian shape $H(t)$ obtained via the Hirota bilinear method [45]. The special case of model (2) with $d(t) = f(t) = 0$ has been converted to the special case of model (1) with $a_1(t) = a(t) + 2b(t)\int H(t)\,dt$, $d_1(t) = a(t)\int H(t)\,dt + 2b(t)[\int H(t)\,dt]^2$ and $f_1(t) = 0$ with the aid of $u = \int H(t)\,dt + q$, with only one-soliton solution obtained via the solitary wave ansätz of the form $A\,\mathrm{sech}^p[k(x - v(t)t)]$ [46]. From the bilinear form of the special case of model (2) with $b(t) = 0$, solitonic propagation and interaction for the special case of model (2) with $b(t) = 0$ have been provided [47].

The integrability plays a role in searching for the analytic solutions of nonlinear evolution equations (NLEEs) [1,12,24]. To our knowledge, integrability aspects of model (2), such as the Painlevé property, Lax pair, and BT, have not been studied. Our main aims in this paper will be to investigate those aspects of model (2). In Sec. II Painlevé-integrable conditions and the Lax pair will be provided. In Sec. III two kinds of the BTs and soliton-like solutions will be obtained. Discussions will be presented in Sec. IV. Conclusions will be given in Sec. V.

II. PAINLEVÉ-INTEGRABLE CONDITIONS AND LAX PAIR

Painlevé analysis is an approach to find the integrable conditions of a given NLEE. In this section, to carry out the Painlevé-integrable conditions, in line with the Weiss-Tabor-Carnevale (WTC) procedure and Kruskal's simplified ansatz [48], we will perform the Painlevé analysis of model (2).

According to the WTC procedure, the generalized Laurent series expansion of u is

$$u = \sum_{j=0}^{\infty} u_j(x,t)\phi(x,t)^{j-\alpha}, \tag{3}$$

where α is a positive integer, and $u_j(x,t)$ are the analytic expansion coefficients in the neighborhood of a movable noncharacteristic singularity manifold $\phi(x,t)$ simplified by $\phi(x,t) = x + \psi(t)$ with $\psi(t)$ as an arbitrary analytic function of t.

For the leading-order analysis, substituting $u \approx u_0\phi^{-\alpha}$ into model (2), and balancing the dominant terms, we obtain $\alpha = 1$ and $u_0 = \pm i[6c(t)/b(t)]^{1/2}\phi_x$. By virtue of symbolic computation, the resonances can be determined as $j = -1, 3, 4$, of which $j = -1$ corresponds to the arbitrariness of the singular manifold $\phi(x,t)$ or $\psi(t)$. We proceed further to find that the compatibility conditions at $j = 3$ and 4 are satisfied identically if and only if the coefficients $a(t)$ and $b(t)$ obey the following constraints:

$$a(t) = c(t)e^{\int f(t)\,dt}\left[m_1 - 2m_2\int e^{\int f(t)dt}H(t)\,dt\right],$$
$$b(t) = m_2 c(t)e^{2\int f(t)\,dt}, \tag{4}$$

where m_1 and m_2 are two arbitrary constants. Therefore, model (2) admits the Painlevé property under conditions (4), namely, the conditions under which the solutions of model (2) are free from the movable singular critical manifold [48]. Constraint conditions (4) under the external force $H(t) = 0$ agree with the conditions for model (1) to pass the Painlevé test [24]. For a damped KdV model, which is a special case of model (2) with $b(t) = 0$, $d(t) = 0$, and $H(t) = 0$, Constraints (4) degenerate into $a(t) = m_1 c(t)e^{\int f(t)\,dt}$ with $m_2 = 0$ corresponding the $b(t) = 0$. With $a(t) = 6$ and $c(t) = 1$, and then $m_1 = 6$ and $f(t) = 0$, the constant-coefficient KdV model come out [1], so that the constant-coefficient damped KdV model does not pass the Painlevé test.

The Lax pair helps people to ensure the complete integrability of a NLEE [49]. To construct a Lax pair of model (2), we introduce the functions $E(x,t)$, $W(t)$, and $G(x,t)$ in the AKNS system [24,49,50], and the Lax pair of model (2) can be expressed as [24,50]

$$\Phi_x = U\Phi = \begin{pmatrix} \lambda & E(x,t)[u + W(t)] \\ G(x,t)Q(x,t) & -\lambda \end{pmatrix}\Phi, \tag{5}$$

$$\Phi_t = V\Phi = \begin{pmatrix} A(x,t,\lambda) & B(x,t,\lambda) \\ F(x,t,\lambda) & -A(x,t,\lambda) \end{pmatrix}\Phi, \tag{6}$$

where the wave function $\Phi = (\Phi_1,\Phi_2)^T$, Φ_1 and Φ_2 are both scalar functions, the superscript T denotes the transpose of the matrix, U and V are two 2×2 null-trace matrices, the eigenvalue λ is a parameter independent of x and t, and $Q(x,t)$, $A(x,t,\lambda)$, $B(x,t,\lambda)$, and $F(x,t,\lambda)$ are the functions of x and t. With respect to λ, expanding $A(x,t,\lambda)$, $B(x,t,\lambda)$, and $F(x,t,\lambda)$ as

$$A(x,t,\lambda) = a_0(x,t) + a_1(x,t)\lambda + a_2(x,t)\lambda^2 + a_3(x,t)\lambda^3, \tag{7}$$

$$B(x,t,\lambda) = b_0(x,t) + b_1(x,t)\lambda + b_2(x,t)\lambda^2, \tag{8}$$

$$F(x,t,\lambda) = f_0(x,t) + f_1(x,t)\lambda + f_2(x,t)\lambda^2, \tag{9}$$

substituting them into the compatibility condition $U_t - V_x + UV - VU = 0$, and equating the like powers of λ, we can obtain 12 equations. The first 10 equations give the expansion coefficients of $A(x,t,\lambda)$, $B(x,t,\lambda)$, and $F(x,t,\lambda)$, and the last two equations give model (2), constraints (4) with $m_2 = 6Q_2$ and $m_1 = 6Q_1 - 12Q_2C_1$, as well as $E(x,t)$, $W(t)$, $G(x,t)$, and $Q(x,t)$ as

$$E(x,t) = e^{gx+\int f(t)\,dt}, W(t) = -e^{-\int f(t)\,dt}(H_f + C_1),$$
$$H_f = \int e^{\int f(t)\,dt}H(t)\,dt, \tag{10}$$

$$G(x,t) = e^{-gx+\int f(t)\,dt},$$
$$Q(x,t) = -Q_1e^{-\int f(t)\,dt} - Q_2u - Q_2W(t), \tag{11}$$

$$\begin{aligned} A(x,t,\lambda) = {} & -d(t)\lambda - 3g^2c(t)\lambda - 2c(t)e^{2\int f(t)\,dt} \\ & \times[3Q_2W(t)u + 2Q(x,t)W(t) - Q(x,t)u]\lambda \\ & + 6gc(t)\lambda^2 - 4c(t)\lambda^3 + \tfrac{1}{2}gd(t) + \tfrac{1}{2}g^3c(t) \\ & + c(t)e^{2\int f(t)\,dt}\times\{Q(x,t)[2gW(t) - gu + u_x] \\ & + Q_2[3gW(t)u + W(t)u_x + uu_x]\}, \end{aligned} \tag{12}$$

$$B(x,t,\lambda) = -4c(t)E(x,t)\,[u+W(t)]\,\lambda^2 + 2c(t)E(x,t)\,[2gW(t)+2gu-u_x]\,\lambda - d(t)E(x,t)[u+W(t)] + 2c(t)E(x,t)Q(x,t)e^{2\int f(t)dt}\,[u+W(t)]^2 + c(t)E(x,t) \times \{-g^2[u+W(t)] + gu_x - u_{xx} - 6W(t)e^{2\int f(t)dt}[u+W(t)][Q_2u+Q(x,t)]\}, \tag{13}$$

$$F(x,t,\lambda) = -4c(t)G(x,t)Q(x,t)\lambda^2 + 2c(t)G(x,t)\,[2gQ(x,t)-Q_2u_x]\,\lambda - d(t)G(x,t)Q(x,t) + 2c(t)G(x,t)Q(x,t)^2e^{2\int f(t)dt}\,[u-2W(t)] + c(t)G(x,t) \times [-g^2Q(x,t) - 6Q_2W(t)e^{2\int f(t)dt}Q(x,t)u + Q_2(gu_x+u_{xx})], \tag{14}$$

where g, C_1, Q_1, and Q_2 are the arbitrary parameters, of which Q_1 and Q_2 correspond with the quadratic and cubic nonlinear coefficients under Painlevé conditions (4) with $m_2 = 6Q_2$ and $m_1 = 6Q_1 - 12Q_2C_1$. Direct calculation shows that model (2) can be obtained from the compatibility condition $U_t - V_x + [U,V] = 0$ of Lax pair (5) and (6) with Eqs. (10)–(14). Under $g = W(t) = 0$ and $Q(x,t) = -Q_2u$, Eq. (5) is the spatial part of the Lax pair of the mKdV model [23]. Equations (5) and (6) with $g = W(t) = 0$ are the Lax pair for model (1) and agree with the corresponding results in Ref. [24].

III. BT AND SOLITON-LIKE SOLUTIONS

BT, originating in the study of differential geometry, is a method for constructing the solutions of NLEEs [8,24,51]. From a seed solution of a NLEE, one can construct other solutions of the NLEE, which can give a transformation between the (N-1)-soliton solutions and the N-soliton solutions [8,24,51].

To construct a BT of model (2), we will use the method in Refs. [8,12,24,50] and introduce a function $\Gamma = \frac{\Phi_1}{\Phi_2}$. Then, Lax pair (5) and (6) about the wave function Φ of model (2) will be reduced to the following equivalent Γ-Riccati system (or Γ system):

$$\begin{aligned}\Gamma_x &= e^{gx+\int f(t)dt}\,[u+W(t)] + 2\lambda\Gamma - e^{-gx+\int f(t)dt}\big[-Q_1e^{-\int f(t)dt} - Q_2u - Q_2W(t)\big]\Gamma^2,\\ \Gamma_t &= B(x,t,\lambda) + 2A(x,t,\lambda)\Gamma - F(x,t,\lambda)\Gamma^2.\end{aligned} \tag{15}$$

The Γ-Riccati-type (Γ-R) BT of model (2) is defined as follows [12,24]:

$$\Gamma' = \Gamma'[\lambda, X(x,t), \Gamma], \quad u' = u + U[\lambda, X(x,t), \Gamma], \tag{16}$$

where Γ' and Γ are two different solutions of Γ-Riccati system (15), u' and u are two distinct solutions of model (2), and $X(x,t)$ is an as-yet-undetermined function.

Under the forms invariant of Γ-Riccati system (15), the transformations can be gained as

$$\Gamma' = \frac{-2e^{gx}\lambda - Q_1\Gamma}{Q_1 - 2Q_2e^{-gx}\lambda\Gamma}, \tag{17}$$

$$u' = u - 2e^{-\int f(t)dt}\left[\frac{gQ_1e^{2gx}\lambda - 4gQ_2e^{gx}\lambda^2\Gamma - gQ_1Q_2\lambda\Gamma^2}{\left(Q_1^2 + 4Q_2\lambda^2\right)(e^{2gx} + Q_2\Gamma^2)} - \frac{e^{gx}\Gamma_x}{e^{2gx} + Q_2\Gamma^2}\right], \tag{18}$$

Eq. (17) and (18) constitute a Γ-R BT of model (2), in which the primed quantities refer to the N-soliton solutions and the unprimed quantities refer to the $(N-1)$-soliton solutions.

Furthermore, with the condition $g = 0$, in line with this procedure and iterating Γ-R BT (18) n times, we can present the following nth-iterated transformation between the old solution u and a new solution u_n of model (2):

$$u_n = u - 2e^{-\int f(t)dt}\frac{\Gamma_n(\lambda_j)_x}{1 + Q_2\Gamma_n(\lambda_j)^2}, \tag{19}$$

where $\Gamma_n(\lambda_j)$ is a solution of Γ-Riccati system (15) corresponding to λ_j ($j = 1,2,3,\ldots,n$) for the solution u_{n-1} ($n = 1,2,3,\ldots,u_0 = u$). Expression (19) with Γ-Riccati system (15) provides us with a procedure to generate the multisoliton-like solutions u_n from a seed solution u of model (2).

Based on symbolic computation, with the condition $g = 0$, solving Γ-R BT (18) for the function Γ, we find the following Γ-u relation:

$$\Gamma = \frac{1}{\sqrt{Q_2}}\tan\left[-\frac{1}{2}\sqrt{Q_2}e^{\int f(t),dt}\int(u'-u)\,dx + \sqrt{Q_2}C_\Gamma(t)\right], \tag{20}$$

where $C_\Gamma(t)$ is an analytic function. Substituting Γ-u relation (20) with $u' = -w'_x$ and $u = -w_x$ (w' and w are the functions of x and t) into Γ-Riccati system (15), we can obtain the following spatial part of the Wahlquist-Estabrook-type Bäcklund transformation (WE-BT) [52]:

$$w'_x + w_x = e^{-\int f(t)\,dt}\left(\frac{2\lambda}{\sqrt{Q_2}}\sin\Theta - \frac{Q_1}{Q_2}\cos\Theta + \frac{Q_1}{Q_2} - 2C_1 - 2H_f\right), \tag{21}$$

with

$$\Theta = \sqrt{Q_2}\big[e^{\int f(t)\,dt}(w' - w) + 2C_\Gamma(t)\big]. \tag{22}$$

With the same procedure, from the time evolution part of Γ-Riccati system (15), the time part of the WE-BT of model (2) can be obtained as

$$\begin{aligned} w'_t + w_t = {} & \frac{4\lambda c(t)}{\sqrt{Q_2}}\left[\frac{Q_1}{2\lambda}w_{xx} - Q_2 e^{\int f(t)\,dt}w_x^2 + R_2 w_x - \frac{R_1}{2c(t)}e^{-\int f(t)\,dt}\right]\sin\Theta \\ & + \frac{2Q_1 c(t)}{Q_2}\left[\frac{2Q_2\lambda}{Q_1}w_{xx} + Q_2 e^{\int f(t)\,dt}w_x^2 - R_2 w_x + \frac{R_1}{2c(t)}e^{-\int f(t)\,dt}\right]\cos\Theta \\ & + \frac{2c(t)}{Q_2}\left(Q_1^2 + 4Q_2\lambda^2\right)w_x - [2xH(t) + f(t)(w' + w) + 2C_\Gamma(t)' e^{-\int f(t)\,dt}] - \frac{1}{Q_2}e^{-\int f(t)\,dt}R_1 R_2, \end{aligned} \tag{23}$$

with

$$R_1 = d(t) + 4c(t)[C_1(Q_1 - C_1 Q_2) + (Q_1 - 2C_1 Q_2)H_f - Q_2 H_f^2 + \lambda^2], \tag{24}$$

$$R_2 = (Q_1 - 2C_1 Q_2 - 2Q_2 H_f). \tag{25}$$

Equations (21) and (23) with Eqs. (22), (24), and (25) constitute a WE-BT of model (2), degenerating into the corresponding results in Ref. [24] for model (1) with $C_1 = C_\Gamma(t) = 0$.

Analytic multisoliton solutions help people to explain the nonlinear wave phenomena [1,7–9,12]. We hereby present the one- or two-soliton-like solutions of model (2) as follows:

With $u = e^{-\int f(t)\,dt}[\int e^{\int f(t)\,dt}H(t)dt + C_1]$ as a seed solution, from the spatial part of Γ-Riccati system (15), the function Γ_1 is obtained as

$$\Gamma_1 = \frac{(g - 2\lambda_1)e^{gx}}{Q_1 + (g - 2\lambda_1)e^{x(g-2\lambda_1)}C_{\Gamma 1}(t)}. \tag{26}$$

Solving the time part of Γ-Riccati system (15) with (26) for $C_{\Gamma 1}(t)$, and then substituting Γ_1 into Γ-R-BT (18) or (19) with $n = 1$ and $g = 0$, we get the one-soliton-like solutions of model (2),

$$u_1 = e^{-\int f(t)\,dt}\left[\int e^{\int f(t)\,dt}H(t)\,dt + C_1 - \frac{16\lambda_1^3 C_{\Gamma 1}e^{\xi_1}}{4\lambda_1^2 C_{\Gamma 1}^2 - 4Q_1\lambda_1 C_{\Gamma 1}e^{\xi_1} + \left(Q_1^2 + 4Q_2\lambda_1^2\right)e^{2\xi_1}}\right], \tag{27}$$

with

$$\xi_1 = 2\lambda_1 x + \omega_1(t) + \xi_{01}, \tag{28}$$

$$\omega_1(t) = -2\lambda_1\int\left[d(t) + c(t)\left(4\lambda_1^2 + 6C_1(Q_1 - Q_2 C_1) + 6(Q_1 - 2Q_2 C_1)H_f - 6Q_2 H_f^2\right)\right]dt, \tag{29}$$

where λ_1, $C_{\Gamma 1}$, and ξ_{01} are the real constants. One-soliton-like solutions (27) under Painlevé conditions (4) with $m_2 = 6Q_2$ and $m_1 = 6Q_1 - 12Q_2 C_1$ satisfy model (2).

Solutions (27) can be rewritten in the hyperbolic function form as follows:

$$u_1 = e^{-\int f(t)\,dt}\left[\int e^{\int f(t)\,dt}H(t)\,dt + C_1\right] + \frac{4\lambda_1^2 e^{-\int f(t)\,dt}}{Q_1 + \sqrt{Q_1^2 + 4Q_2\lambda_1^2}\cosh\left(e^{\xi_1 + \log\frac{-\sqrt{Q_1^2+4Q_2\lambda_1^2}}{2C_{\Gamma 1}\lambda_1}}\right)}. \tag{30}$$

According to the similar process, from Γ-Riccati system (15) for Γ_2, the two-soliton-like solutions of model (2) are expressed as follows:

$$u_2 = e^{-\int f(t)\,dt}\left[H_f + C_1 + \frac{8(a_1 e^{\xi_1} + a_2 e^{\xi_2} + a_3 e^{2\xi_1+\xi_2} + a_4 e^{\xi_1+2\xi_2} + a_5 e^{\xi_1+\xi_2})}{(1 + b_1 e^{\xi_1} + b_2 e^{\xi_2} + b_3 e^{\xi_1+\xi_2})(1 + d_1 e^{\xi_1} + d_2 e^{\xi_2} + d_3 e^{\xi_1+\xi_2})}\right], \tag{31}$$

with

$$\xi_2 = 2\lambda_2 x + \omega_2(t) + \xi_{02}, \tag{32}$$

$$\omega_2(t) = -2\lambda_2 \int \left[d(t) + c(t)\left(4\lambda_2^2 + 6C_1(Q_1 - Q_2C_1) + 6(Q_1 - 2Q_2C_1)H_f - 6Q_2H_f^2\right)\right] dt, \tag{33}$$

$$P_j = Q_1 - 2\lambda_j\sqrt{Q_2}, \quad S_j = Q_1 - i2\lambda_j\sqrt{Q_2}, \quad V_j = Q_1 + i2\lambda_j\sqrt{Q_2}, \quad j = 1,2, \tag{34}$$

$$a_1 = \frac{\lambda_1^2}{P_1}, \quad a_2 = \frac{\lambda_2^2}{P_2}, \quad a_3 = \frac{(\lambda_1 - \lambda_2)^2\lambda_2^2 S_1 V_1}{(\lambda_1 + \lambda_2)^2 P_1^2 P_2}, \quad a_4 = \frac{(\lambda_1 - \lambda_2)^2\lambda_1^2 S_2 V_2}{(\lambda_1 + \lambda_2)^2 P_1 P_2^2}, \quad a_5 = 2Q_1\frac{(\lambda_1 - \lambda_2)^2}{P_1 P_2}, \tag{35}$$

$$b_1 = \frac{S_1}{P_1}, \quad b_2 = \frac{S_2}{P_2}, \quad b_3 = \frac{(\lambda_1 - \lambda_2)^2\lambda_2^2 S_1 S_2}{(\lambda_1 + \lambda_2)^2 P_1 P_2}, \quad d_1 = \frac{V_1}{P_1}, \quad d_2 = \frac{V_2}{P_2} \quad d_3 = \frac{(\lambda_1 - \lambda_2)^2\lambda_1^2 V_1 V_2}{(\lambda_1 + \lambda_2)^2 P_1 P_2}, \tag{36}$$

where λ_2 and ξ_{02} are the real constants. Two-soliton-like solutions (31) with Eqs. (28), (29), and (32)–(36) under Painlevé conditions (4) with $m_2 = 6Q_2$ and $m_1 = 6Q_1 - 12Q_2C_1$ satisfy model (2). Similarly, the N-soliton-like solutions can also be constructed.

IV. DISCUSSION

From the integrable aspects, we have investigated model (2) in plasmas and fluids with the inhomogeneities of media and nonuniformities of boundaries, and presented the soliton-like solutions, based on which the effects of the inhomogeneous coefficients, external force term, eigenvalue, and certain parameters on the solitonic propagation and interaction will be discussed.

For the ion-acoustic wave in the vicinity of the negative-ion critical density, inhomogeneous coefficients of model (2) can be expressed as [9]

$$a(t) = \frac{1}{2}\left(3\frac{n_{\alpha 0}}{V^4} - 3\frac{n_{\beta 0}}{Q^2V^4} - 1\right),$$
$$b(t) = \frac{1}{4}\left(15\frac{n_{\alpha 0}}{V^6} + 15\frac{n_{\beta 0}}{Q^3V^6} - 1\right), \tag{37}$$
$$c(t) = \frac{1}{2}, \quad d(t) = 0, \quad f(t) = 0,$$
$$V = \sqrt{n_{\alpha 0} + \frac{n_{\beta 0}}{Q^2}}, \; Q = \frac{m_\beta}{m_\alpha}, \tag{38}$$

where $n_{\alpha 0}$ and $n_{\beta 0}$ denote the positive and negative ion densities normalized by the electron density, respectively, and m_α and m_β are the positive and negative ion masses, respectively.

For a two-layer system in the Boussinesq approximation, inhomogeneous coefficients of model (2) can be expressed as [22]

$$a(t) = 3d(t)\frac{h_1 - h_2}{2h_1h_2}, \quad b(t) = -\frac{3d(t)}{8h_1^2h_2^2}\left(h_1^2 + h_2^2 + 6h_1h_2\right),$$
$$c(t) = \frac{d(t)h_1h_2}{6}, \tag{39}$$
$$d(t) = \sqrt{g\sigma\frac{h_1h_2}{h_1 + h_2}}, \quad f(t) = k, \quad \sigma = \frac{2(\rho_2 - \rho_1)}{\rho_2 + \rho_1}, \tag{40}$$

where g is the gravitational acceleration, k is an arbitrary constant, h_1 and h_2 denote the mean upper and lower layer depths, respectively, and ρ_1 and ρ_2 are the densities of the upper and lower layers, respectively.

In line with Refs. [14,16,20,21], the amplitude A_j (peak value) of each solitary wave can be

$$A_j = \frac{4\lambda_j^2}{Q_1(1 + B)}e^{-\int f(t)\,dt}, \quad B^2 = 1 + \frac{4Q_2}{Q_1^2}\lambda_j^2,$$
$$\text{or } Q_2 = \frac{(B^2 - 1)Q_1^2}{4\lambda_j^2}. \tag{41}$$

By the aid of the characteristic-line method [45,47], the velocity v_j of each solitary wave can be expressed as

$$v_j(t) = d(t) + c(t)\left(4\lambda_j^2 + m_1C_1 + m_2C_1^2 + m_1H_f - m_2H_f^2\right),$$
$$H_f = \int e^{\int f(t)\,dt} H(t)\,dt. \tag{42}$$

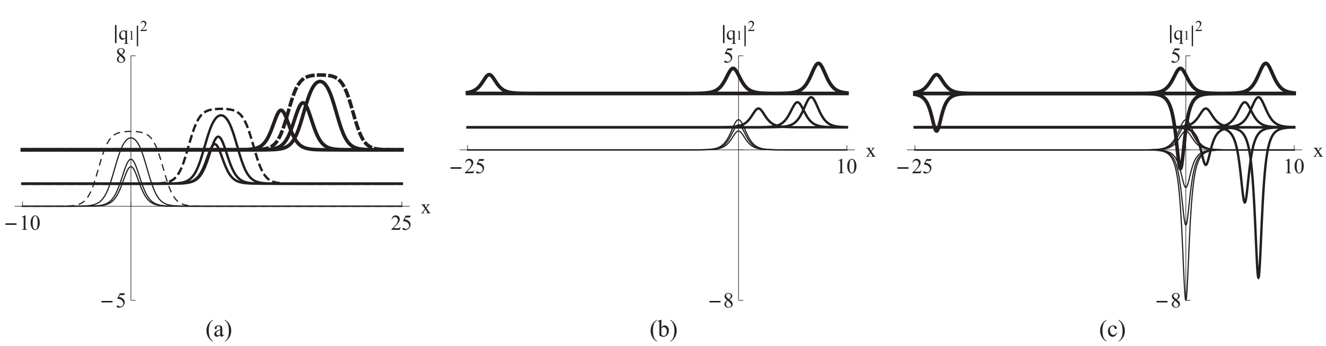

FIG. 1. Soliton-like solutions via expression (30) with the parameters $c(t) = \lambda_j = Q_1 = 1$, $d(t) = f(t) = C_1 = 0$, (a) $Q_2 < 0$, $B = 0.9/0.6/0.1/0.005$ (dashed), $H(t) = t$, $t = 0$ (thin), $H(t) = 1.2t$, $t = 1$ (middle), $H(t) = 3t$, $t = 1$ (thick); (b) $Q_2 > 0$, $B = 1.5/2/3$ (small amplification), $H(t) = t$, $t = 0$ (thin), $H(t) = 1.2t$, $t = 1$ (middle), $H(t) = 3t$, $t = 1$ (thick); (c) $Q_2 > 0$, $B = -1.5/-2/-3$, $H(t) = t$, $t = 0$ (thin), $H(t) = 1.2t$, $t = 1$ (middle), $H(t) = 3t$, $t = 1$ (thick), superposed on (b).

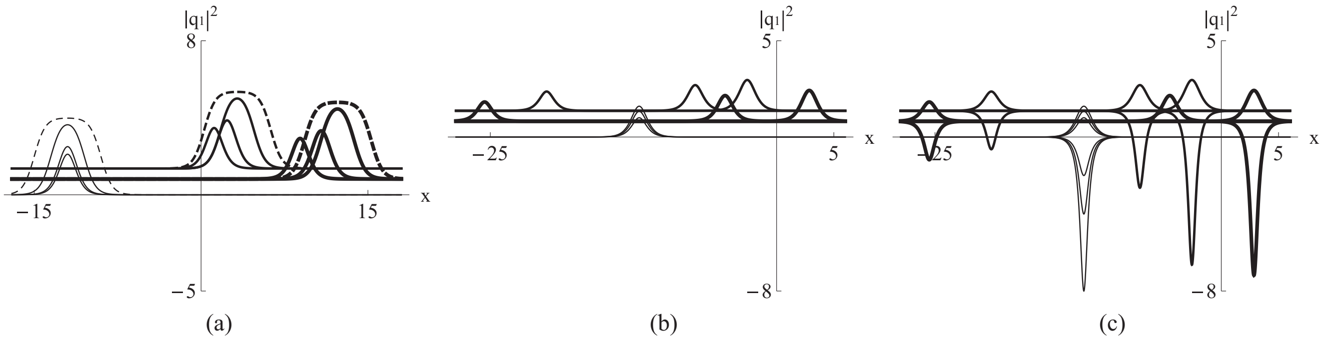

FIG. 2. Soliton-like solutions via expression (30) with the parameters $c(t) = \lambda_j = Q_1 = 1$, $d(t) = C_1 = 0$, $H(t) = 2$, (a) $Q_2 < 0$, $B = 0.9/0.6/0.1/0.005$ (dashed), $f(t) = t$, $t = 0$ (thin), $f(t) = 1.2t$, $t = 1$ (middle), $f(t) = 3t$, $t = 1$ (thick); (b) $Q_2 > 0$, $B = 1.5/2/3$ (small amplification), $f(t) = t$, $t = 0$ (thin), $f(t) = 1.2t$, $t = 1$ (middle), $f(t) = 3t$, $t = 1$ (thick); (c) $Q_2 > 0$, $B = -1.5/-2/-3$, $f(t) = t$, $t = 0$ (thin), $f(t) = 1.2t$, $t = 1$ (middle), $f(t) = 3t$, $t = 1$ (thick), superposed on (b).

It can be noticed that the dispersive coefficient $c(t)$, dissipative coefficient $d(t)$, linear-damping coefficient $f(t)$, and external force $H(t)$ can all influence the propagation velocity of the solitons, and parameters Q_1, Q_2, C_1 and eigenvalue λ_j can also influence the propagation properties of the soliton-like solutions. On the other hand, Q_1, $B(Q_2)$, λ_j, and $f(t)$ can affect the peak value A_j. By means of taking the different choices of Q_2 and $B(Q_2)$ in Eqs. (41) and (42), the influence will be illustrated in Figs. 1–3.

(1) When $Q_2 < 0$ and $0 < B(Q_2) < 1$: The soliton-like shape and propagation are shown in Figs. 1(a), 2(a), and 3(a). $B \to 1$ (namely, $Q_2 \to 0$) corresponds to a small wave amplitude, and the soliton-like solutions of model (2) reduce to the solitary waves of the KdV model corresponding to the results in Ref. [47]. $B \to 0$ represents the critical value $A_{\max} = \frac{Q_1}{|Q_2|} e^{-\int f(t)\,dt}$ at which the widths of the soliton-like solutions increase to infinity. It can be seen that the external force $H(t)$ affects the wave velocity and wave background in Fig. 1(a) (C_1 has the similar effect with a different ratio), that the linear-damping coefficient $f(t)$ influences the initial center position, velocity, and background of solitons in Fig. 2(a), and that the dispersive coefficient $c(t)$ works only on the wave velocity with the $H(t) = 2$ affecting the wave background in Fig. 3(a) [the dissipative coefficient $d(t)$ has the similar influence].

(2) When $Q_2 > 0$ and $1 < B(Q_2) < \infty$: Figs. 1(b), 2(b), and 3(b) portray the soliton-like shape and character of propagation (including the speed and moving direction). It is clear that the soliton-like solutions with different values of B are superposed at $t = 0$ and separate gradually with different speed and moving directions as t increases. Similarly, the external force $H(t)$ affects the wave velocity and wave background in Fig. 1(b), the linear-damping coefficient $f(t)$ influences the initial center position, the velocity, and background with bidirectional changing of the soliton-like solutions in Fig. 2(b), and the dispersive coefficient $c(t)$ works only on the wave velocity with $H(t) = 2$ affecting the wave background in Fig. 3(b). When $Q_2 > 0$ and $-\infty < B(Q_2) < -1$, the soliton-like shape is reversed, and the character of propagation is coincident with $1 < B(Q_2) < \infty$ [as seen in Figs. 1(c), 2(c) and 3(c) in which the curves with $H(t) = 3t$ and $B = -1.5$, $f(t) = 3t$ and $B = -2$, and $c(t) = 3t$ and $B = -2$ are not drawn for clarity].

Hereafter, we devote our effort to investigate the effects of external force $H(t)$ and parameter C_1 on the interaction of the solitons.

(1) When the external force $H(t) = 0$ and parameter C_1 has different choices: Fig. 4(a) shows that the trajectories of the two-soliton-like solutions are two parabolic-typed curves with the unchangeable amplitudes and oscillation in the local region

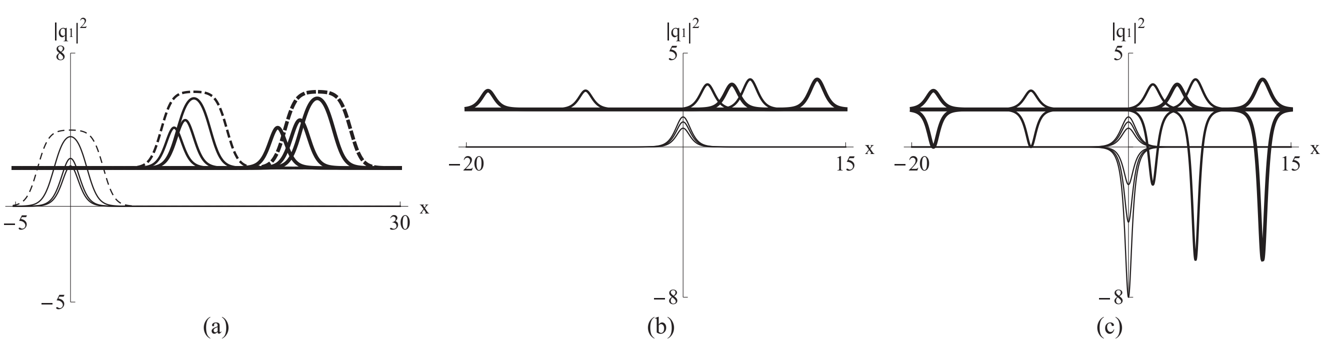

FIG. 3. Soliton-like solutions via expression (30) with the parameters $\lambda_j = Q_1 = 1$, $d(t) = f(t) = C_1 = 0$, $H(t) = 2$, (a) $Q_2 < 0$, $B = 0.9/0.6/0.1/0.005$ (dashed), $c(t) = t$, $t = 0$ (thin), $c(t) = 1.5t$, $t = 1$ (middle), $c(t) = 3t$, $t = 1$ (thick); (b) $Q_2 > 0$, $B = 1.5/2/3$ (small amplification), $c(t) = t$, $t = 0$ (thin), $c(t) = 1.5t$, $t = 1$ (middle), $c(t) = 3t$, $t = 1$ (thick); (c) $Q_2 > 0$, $B = -1.5/-2/-3$, $c(t) = t$, $t = 0$ (thin), $c(t) = 1.5t$, $t = 1$ (middle), $c(t) = 3t$, $t = 1$ (thick), superposed on (b).

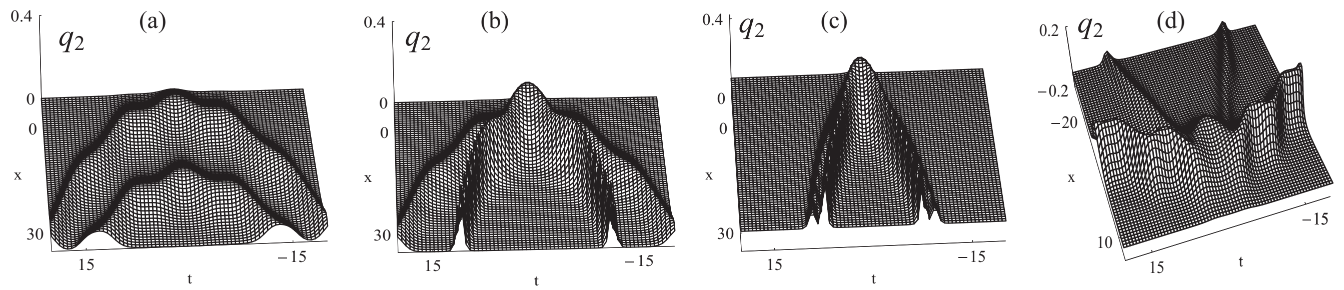

FIG. 4. Two-soliton-like solutions via expression (31) with $c(t) = t$, $d(t) = \sin(0.8t)$, $f(t) = H(t) = 0$, $Q_1 = -Q_2 = 1$, $\lambda_1 = 0.2$. (a) $C_1 = 0$, $\lambda_2 = 0.21$; (b) $C_1 = 0$, $\lambda_2 = 0.35$; (c) $C_1 = 0.1$, $\lambda_2 = 0.35$; (d) $C_1 = -0.1$, $\lambda_2 = 0.35$.

for $c(t) = t$ and $d(t) = \sin(0.8t)$, and have no interaction for the small differences between the eigenvalues $\lambda_1 = 0.2$ and $\lambda_2 = 0.21$. On the other hand, Figs. 4(b), 4(c), and 4(d) show that the tracks of the two-soliton-like solutions are also two parabolic-like curves, but have the interaction for the relatively-large difference between the eigenvalues $\lambda_1 = 0.2$ and $\lambda_2 = 0.35$. In contrast to Fig. 4(b), it can be noticed that the background goes up for $C_1 = 0.1$ in Fig. 4(c) with less vibration and two smaller spans of time on the two parabolic-typed trajectories, and drops down for $C_1 = -0.1$ in Fig. 4(d) with more vibration and larger time-scale propagation trajectories. Furthermore, with $C_1 = 1$, the two-soliton-like solutions will be syncretized to the one-soliton-like solution with smoother unchangeable amplitude and smaller time scale on the parabolic-typed trajectory.

(2) When the external force $H(t) = -0.1e^{-0.25t^2}$ and parameter C_1 has some choices: Fig. 5 presents the development of the two-soliton-like solutions with some vibration for $d(t) = \sin(0.8t)$ on the shock wave background for the external force $H(t) = -0.1e^{-0.25t^2}$, but no interacting section and amplitude change for the small difference between the eigenvalues $\lambda_1 = 0.35$ and $\lambda_2 = 0.355$. The evolution directions of the two-soliton-like solutions have changed to the positive x axis direction, and the plane wave background has moved up for $C_1 = 1$ in Fig. 5(b). However, the propagation directions of the two-soliton-like solutions have rotated to the negative x axis direction, and the plane wave background has declined for the opposite value $C_1 = -0.3$ in Fig. 5(c). On the other hand, Fig. 6 shows the interaction development of the two-soliton-like solutions for the differentiation between $\lambda_1 = 0.35$ and $\lambda_2 = 0.6$. When $C_1 = 0$, it can be seen that the propagation directions of the two-soliton-like solutions have a change on the shock wave background for $H(t) = -0.1e^{-0.25t^2}$ in Fig. 6(a). With $C_1 = 0.5$, the propagation directions of the two-soliton-like solutions hold unchangeable except for the phase [as seen in Fig. 6(b)]. In comparison, the propagation directions of the two-soliton-like solutions turn more to the negative x axis direction with the inverse parameter $C_1 = -0.5$.

V. CONCLUSIONS

The generalized inhomogeneous model (2) in certain plasmas and stratified fluids has been investigated. Making use of the Painlevé analysis, we have obtained Painlevé integrable conditions (4) of model (2), under which Lax pair (5) and (6), Γ-R BT (18) or (19), and WE-BT (21) and (23) have been presented. Based on the Γ-R BT, analytic one- or two-soliton-like solutions (30) and (31) with all the inhomogeneous coefficients $a(t)$,$b(t)$,$c(t)$,$d(t)$, $f(t)$, external force $H(t)$, eigenvalues λ'_j, and another parameter C_1 have been constructed, of which the quadratic coefficient $a(t)$ and the cubic nonlinear coefficient $b(t)$ correspond to the parameters Q_1 and Q_2 under Painlevé integrable conditions (4) with $m_2 = 6Q_2$ and $m_1 = 6Q_1 - 12Q_2C_1$, respectively. By the aid of expressions (41), it has been understood that the amplitudes of solitons are influenced by the eigenvalues λ'_j in Lax pair (5) and (6), the linear-damping coefficient $f(t)$, and the parameters Q_1 and Q_2 (as seen in Figs. 1–3). By virtue of the characteristic-line method, velocity (42) has implied that the inhomogeneous coefficients $c(t)$,$d(t)$, $f(t)$, external force $H(t)$, eigenvalues λ'_j, and parameters Q_1, Q_2, C_1 will influence the solitonic velocity (as seen in Figs. 1–3). From the graphic illustration shown in Figs. 4–6, the solitonic propagation and

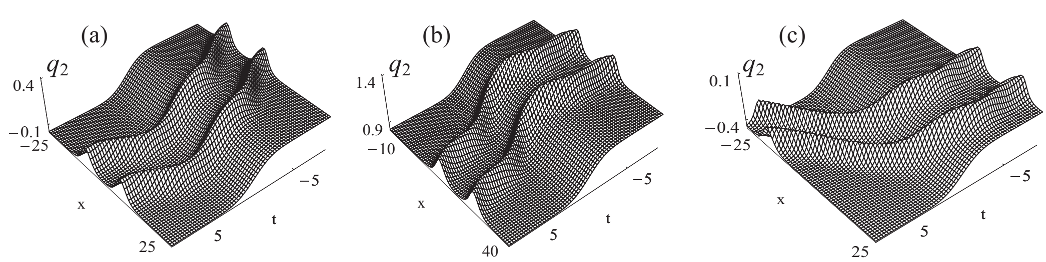

FIG. 5. Two-soliton-like solutions via expression (31) with $c(t) = 1$, $d(t) = \sin(0.8t)$, $f(t) = 0$, $H(t) = -0.1e^{-0.25t^2}$, $Q_1 = Q_2 = 1$, $\lambda_1 = 0.35$, $\lambda_2 = 0.355$, (a) $C_1 = 0$; (b) $C_1 = 1$; (c) $C_1 = -0.3$.

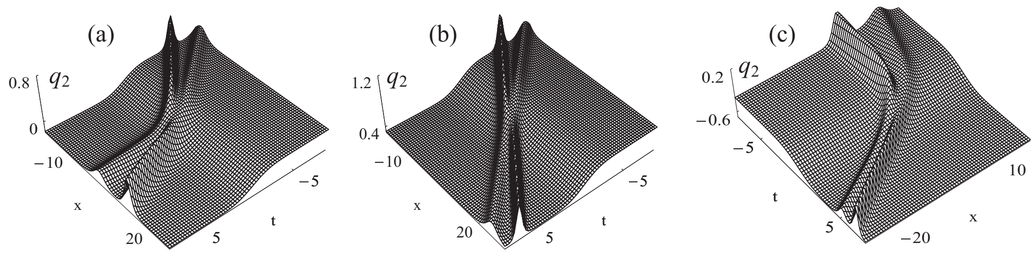

FIG. 6. Two-soliton-like solutions via expression (31) with $c(t) = d(t) = 1$, $f(t) = 0$, $H(t) = -0.1e^{-0.25t^2}$, $Q_1 = Q_2 = 1$, $\lambda_1 = 0.35$, $\lambda_2 = 0.6$, (a) $C_1 = 0$; (b) $C_1 = 0.5$; (c) $C_1 = -0.5$.

interaction of model (2) have been presented with the facts that the solitonic background is affected by the linear-damping coefficient $f(t)$, external force $H(t)$, and another parameter C_1, and the degree of solitonic infection is sensitive to the eigenvalues λ'_j.

ACKNOWLEDGMENTS

This work has been supported by the National Natural Science Foundation of China under Grant Nos. 11074020, 11272023, and 61072145.

[1] M. J. Ablowitz and P. A. Clarkson, *Solitons, Nonlinear Evolution Equations and Inverse Scattering* (Cambridge University Press, Cambridge, 1992).
[2] V. D. DjorDjevic and L. G. Redekopp, J. Phys. Oceanography **8**, 1016 (1978); P. E. Holloway, E. Pelinovsky, T. Talipova, and B. Barnes, *ibid.* **27**, 871 (1997); T. G. Talipova, E. N. Pelinovskii, and T. Kouts, Oceanology **38**, 33 (1998).
[3] Z. Horii, Phys. A **337**, 398 (2004); Q. Han, L. Dai, and M. Dong, Commun. Nonl. Sci. Numer. Simulat. **10**, 607 (2005).
[4] H. Washimi and T. Taniuti, Phys. Rev. Lett. **17**, 996 (1966); R. J. Taylor, D. R. Baker, and H. Ikezi, *ibid.* **24**, 206 (1970); H. Ikezi, Phys. Fluids **16**, 1668 (1973).
[5] G. C. Das and S. G. Tagare, Plasma Phys. **17**, 1025 (1975).
[6] J. Mason and E. Knobloch, Phys. D **205**, 100 (2005); L. P. Zhang and J. K. Xue, Chaos Solitons Fract. **23**, 543 (2005).
[7] Y. T. Gao and B. Tian, Phys. Plasmas **13**, 112901 (2006); **13**, 120703 (2006).
[8] M. Wadati, J. Phys. Soc. Jpn. **38**, 673 (1975); **38**, 681 (1975).
[9] S. Watanabe, J. Phys. Soc. Jpn. **53**, 950 (1984); **44**, 611 (1978); J. Plasma Phys. **14**, 353 (1975).
[10] K. Konno and Y. H. Ichikawa, J. Phys. Soc. Jpn. **37**, 1631 (1974); K. Konno and M. Wadati, Prog. Theor. Phys. **53**, 1652 (1975).
[11] Y. Nejoh, Phys. Fluids B **4**, 2830 (1992).
[12] A. H. Khater, A. A. Abdallah, and O. H. El-Kalaawy, Phys. Plasmas **6**, 4542 (1999).
[13] H. L. Liu and M. Slemrod, Appl. Math. Lett. **17**, 401 (2004).
[14] R. Grimshaw, E. Pelinovaky, T. Talipova, and A. Kurlin, J. Phys. Oceanography **34**, 2774 (2004); R. Grimshaw, E. Pelinovsky, and T. Talipova, Wave Motion **37**, 351 (2003).
[15] K. G. Lamb and L. Yan, J. Phys. Oceanography **26**, 2712 (1996).
[16] O. Nakoulima, N. Zahibo, E. Pelinovsky, T. Talipova, A. Slunyaev, and A. Kurkin, Appl. Math. Comput. **152**, 449 (2004).
[17] R. J. Small and R. P. Hornby, Ocean Modelling **8**, 395 (2005).
[18] J. W. Miles, Tellus **31**, 456 (1979); **33**, 397 (1981).
[19] J. A. Gear and R. Grimshaw, Phys. Fluids **26**, 14 (1983).
[20] R. Grimshaw, E. Pelinovsky, and T. Talipova, Phys. D **132**, 40 (1999); **159**, 35 (2001); R. Grimshaw, D. Pelinovsky, E. Pelinovsky, and A. Slunyaev, Chaos **12**, 1070 (2002).
[21] A. V. Slyunyaev, J. Exp. Theor. Phys. **92**, 529 (2001).
[22] K. R. Helfrich and W. K. Melville, Annu. Rev. Fluid Mech. **38**, 395 (2006).
[23] Y. Zhang, J. Li, and Y. N. Lv, Ann. Physics **323**, 3059 (2008); H. Y. Nguyen and F. Dias, Phys. D **237**, 2365 (2008).
[24] J. Li, T. Xu, X. H. Meng, Ya. X. Zhang, H. Q. Zhang, and B. Tian, J. Math. Anal. Appl. **336**, 1443 (2007).
[25] L. H. Zhang, L. H. Dong, and L. M. Yan, Appl. Math. Comput. **203**, 784 (2008).
[26] X. G. Xu, X. H. Meng, Y. T. Gao, and X. Y. Wen, Appl. Math. Comput. **210**, 313 (2009).
[27] W. R. Shan and B. Tan, Commun. Nonl. Sci. Numer. Simulat. **17**, 4559 (2012).
[28] T. Kakutani and N. Yamasaki, J. Phys. Soc. Jpn. **45**, 674 (1978).
[29] B. Dey, J. Phys. A **19**, L9 (1986).
[30] B. A. Malomed and V. I. Shrira, Phys. D **53**, 1 (1991).
[31] B. Li, Y. Chen, and H. Q. Zhang, Phys. Lett. A **305**, 377 (2002).
[32] A. M. Wazwaz, Communi. Nonl. Sci. Numer. Simul. **12**, 1395 (2007).
[33] M. N. B. Mohamad, Math. Methods Appl. Sci. **15**, 73 (1992).
[34] Y. Z. Peng, I. J. Theor. Phys. **42**, 863 (2003).
[35] J. F. Zhang, I. J. Theor. Phys. **37**, 1541 (1998).
[36] Sirendaoreji, Phys. Lett. A **356**, 124 (2006).
[37] H. Triki, T. R. Taha, and A. M. Wazwaz, Math. Compu. Simul. **80**, 1867 (2010).
[38] W. P. Hong and M. S. Yoon, Z. Naturforsch. A **56**, 366 (2001).
[39] E. G. Fan, Chaos Solitons Fract. **16**, 819 (2003).
[40] K. R. Helfrich, W. K. Melville, and J. W. Miles, J. Fluid Mech. **149**, 305 (1984); K. R. Helfrich and W. K. Melville, *ibid.* **167**, 285 (1986).
[41] K. W. Chow, R. H. J. Grimshaw, and E. Ding, Wave Motion **43**, 158 (2005).
[42] H. Wu, Y. Zeng, and T. Fan, Commun. Nonl. Sci. Numer. Simulat. **13**, 2146 (2008).

[43] M. Song, X. Hou, and J. Cao, Appl. Math. Comput. **217**, 5942 (2011).
[44] H. Z. Liu, J. Li, and L. Liu, Nonlin. Dyn. **59**, 497 (2010).
[45] Y. Liu, Y. T. Gao, Z. Y. Sun, and X. Yu, Nonlin. Dyn. **66**, 575 (2011).
[46] A. M. Wazwaz, Appl. Math. Comput. **217**, 2277 (2010).
[47] X. Yu, Y.-T. Gao, Z.-Y. Sun, and Y. Liu, Phys. Rev. E **83**, 056601 (2011).
[48] J. Weiss, M. Tabor, and G. Carnevale, J. Math. Phys. **24**, 522 (1983); J. Weiss, *ibid*. **24**, 1405 (1983).
[49] M. J. Ablowitz, D. J. Kaup, A. C. Newell, and H. Segur, Phys. Rev. Lett. **31**, 125 (1973); Stud. Appl. Math. **53**, 249 (1974).
[50] Y. P. Liu, Y. T. Gao, and G. M. Wei, Phys. A **391**, 535 (2012); **392**, 656 (2013).
[51] David Gómez-Ullate, Sara Lombardo, Manuel Mañas, Marta Mazzocco, Frank Nijhoff, and Matteo Sommacal, J. Phys. A **43**, 430301 (2010).
[52] H. D. Wahlquist and F. B. Estabrook, Phys. Rev. Lett. **31**, 1386 (1973).